

AD

INVESTIGATION OF MAIN PARAMETERS OF SILICON CARBIDE THYRISTORS

Final Technical Report

by
M.E. LEVINSHTEIN

October 1998

United States Army

EUROPEAN RESEARCH OFFICE OF THE U.S. ARMY

London, England

CONTRACT NUMBER 68171-97-M-5703

R&D 8236-EE-01

19981119 070

A. F. IOFFE INSTITUTE OF RUSSIAN ACADEMY OF SCIENCES, RUSSIA

DTIC QUALITY INSPECTED 3

Approved for Public Release; distribution unlimited

REPORT DOCUMENTATION PAGE			Form Approved OMB No.0704-0188
1. AGENCY USE ONLY (Leave Blank)	2. REPORT DATE	3. REPORT TYPE AND DATES COVERED	
	05 Oct. 98	Final, Aug. 97 - Oct. 98	
4. TITLE AND SUBTITLE INVESTIGATION OF THE MAIN PARAMETERS OF SILICON CARBIDE THYRISTORS			5. FUNDING NUMBERS
6. AUTHOR(S) M.E. LEVINSHTEIN			
7. PERFORMING ORGANIZATION NAME(S) AND ADDRESS(ES) IOFFE INSTITUTE OF RUSSIAN ACADEMY OF SCIENCES 194021 ST. PETERSBURG, RUSSIA			8. PERFORMING ORGANIZATION REPORT NUMBER
9. SPONSORING/MONITORING AGENCY NAME(S) AND ADDRESS(ES) NAVAL REGIONAL CONTRACTING CENTER DETACHMENT LONDON, BLOCK 2, WING 11, DOE COMPLEX, EASTCOTE ROAD RUISLIP, MIDDX, HA4 8BS			10. SPONSORING/MONITORING AGENCY REPORT NUMBER
11. SUPPLEMENTARY NOTES			
12a. DISTRIBUTION/AVAILABILITY STATEMENT			12b. DISTRIBUTION CODE
13. ABSTRACT (Maximum 200 words) The purpose of this work is to study the main parameters of silicon carbide thyristors. The switch-on processes have been studied within the temperature range from 160K to 500K. It was found that turn on constant τ_r is strongly temperature dependent (at T=495K τ_r is as small as $\tau_r=1.9$ ns for 400V thyristor). The critical charge density in SiC thyristors has been measured for the first time at T=300K-560K. Forward current-voltage characteristics were studied up to very high current density $j=100$ kA/cm ² . The theoretical model was put forward to interpret the experimental current-voltage characteristics. The critical current density j_0 at which the "on" state does not spread and occupies only part of the structure has been determined (j_0 falls in the range from 300A/cm ² to 750A/cm ²). The operation frequency $f=10^6$ Hz at operation current density $j=1.4 \times 10^4$ A/cm ² was achieved. The results obtained are compared with theoretical estimations. As a result of this work all main parameters of SiC thyristors are established			
14. SUBJECT ITEMS			15. NUMBER OF PAGES 21
			16. PRICE CODE
17. SECURITY CLASSIFICATION UNCLASSIFIED	18. SECURITY CLASSIFICATION UNCLASSIFIED	19. SECURITY CLASSIFICATION UNCLASSIFIED	20. LIMITATION OF ABSTRACT

TABLE OF CONTENTS

1. STATEMENT OF THE PROBLEM.

2. BACKGROUND

3. EXPERIMENTAL DETAILS

4. RESULTS AND ANALYSIS

4.1. Turn-on process

4.2. Critical charge density

4.3. Forward current-voltage characteristics

4.4. Turn-on spread

4.5 Frequency limitations

5 CONCLUSIONS AND RECOMMENDATIONS

1. STATEMENT OF THE PROBLEM

The purpose of this work is to investigate the main parameters of silicon carbide thyristors. Thyristor is one of the base elements of modern power semiconductor electronics. SiC thyristors can find use in superhigh voltage and superhigh current systems as well as in high temperature and radiation hard electronics. Silicon carbide based thyristors are expected to show great performance advantages as compared to those made with Si and GaAs. This is because SiC has by an order of magnitude higher breakdown electric field than Si or GaAs. The high breakdown electric field allows design of SiC thyristors with thinner and higher doped base layers than in identically rated Si and GaAs thyristors. Such devices may be expected to show fast switching and low residual voltage drop at very high current densities. The high thermal conductivity of SiC should allow higher current density operation of SiC thyristors. The large bandgap of SiC is also expected to result in a much higher operating temperature and higher radiation hardness than in Si and GaAs thyristors. SiC thyristors have been shown to operate successfully at 800K [1,2]. Hence SiC thyristors could find use in the systems with critical constraints on the size, weight and elevated temperature parameters of power units, especially in military systems.

Before this work, the main parameters of SiC thyristors were not practically investigated.
In this work we study:

The switch-on processes within the temperature range from 160K to 500K.

The critical charge density in SiC thyristors in temperature interval of 300K-560K.

Forward current-voltage characteristics up to current density $j=100 \text{ kA/cm}^2$.

The critical current density j_0 at which the "on"-state does not spread and occupies only part of the structure.

The frequency properties of SiC thyristors.

2. BACKGROUND

The first SiC thyristors were demonstrated in late 80ies [3]. High temperature 4H - SiC thyristors manufactured by CREE Research, Inc., have been demonstrated at the beginning of 90ies[4,5]. These SiC thyristors have been shown to operate successfully at 800K [6].

In spite of the fact that SiC power devices must have advantages as compared with Si and GaAs ones, the first measurements of switch-on processes [7] showed rather moderate results. The switch-on process was characterized by current rise time constant $\tau_r = 43 \text{ nsec}$ and residual voltage drop $V_{do} > 10 \text{ V}$ at forward current density $j_0 = 5 \text{ kA/cm}^2$. Either τ_r or V_{do} in these thyristors are higher than related values for identically rated Si thyristors. These results made questionable practical use of SiC thyristors at high and super high current densities.

Besides several important SiC thyristor parameters, such as the switch-on time constant, current-voltage characteristics at high current density, critical charge density, spread velocity of the turn-on state, were not studied practically before the beginning of this work.

The concept of the critical charge density was put forward in ref. [8] and developed in refs. [9, 10]. The critical charge density of a thyristor determines the maximum voltage ramp (dV/dt) of the thyristor [10], the minimum value of the gate control current density [11], the spread velocity of the "on"- state [12], the holding current, and the parameters of current filamentation in gate-controlled thyristors [13]. However, there were no data on critical charge density in SiC thyristors before the beginning of this work.

It is known there exists a critical current density j_0 at which the turned-on state does not spread and occupies only part of the structure (the spread velocity is equal to zero). Along with critical density charge of the minority carriers n_{cr} , the j_0 defines the maximum voltage ramp (dV/dt) of the thyristors [12]. For GaAs and Si thyristors, the relationship between j_0 and the main parameters of the thyristors

has been investigated very thoroughly. However, there were no data on j_0 value in SiC thyristors before the beginning of this work.

We have previously studied the current rise time constant in 4H-SiC thyristors with the voltage blocking capability 400 V. We discovered also that forward voltage drop in these devices is much less than in rated Si and GaAs thyristors at high and super high (up to 100 kA/cm²) current densities [14].

3. EXPERIMENTAL DETAILS

The device structures of the npnp 4H-SiC thyristors investigated in this work is shown in Fig. 1. A forward blocking voltage V_b is equal to about 400 V and $V_b \sim 700$ V for two different types of the thyristors. Thyristors with a forward blocking voltage $V_b \sim 400$ V had the voltage-blocking p-layer of 4.5 μm thick with acceptor doping concentration $N_a - N_d = 2.8 \cdot 10^{16} \text{ cm}^{-3}$. The n-base had a thickness of 0.55 μm and a doping concentration of $4.5 \cdot 10^{17} \text{ cm}^{-3}$. The active area of the devices was $S = 3.6 \cdot 10^{-4} \text{ cm}^2$. Thyristors with a forward blocking voltage $V_b \sim 700$ V had the thickness of the voltage blocking base (p-base) $W_p = 11 \mu\text{m}$. The n-base had a thickness W_n of 0.65 μm . The operating area of the device S was about $4.5 \cdot 10^{-3} \text{ cm}^2$. The thyristors were encapsulated in standard TO-220 packages. The parasitic inductance of the package was 10 to 12 nH.

Turn-on process.

The turn-on process was investigated in the circuit shown in Fig. 2. The capacitor C_0 ($10 \text{nF} < C_0 < 100 \text{nF}$) was charged to a voltage V_0 through a 200 k Ω resistance (R_1). The device was turned-on by 3-200 nsec gate pulse. The load resistance (R_L) was varied in the 1.1 Ω - 50 Ω range to obtain the desired operating current density. The parasitic inductance value of the circuit was not more than 0.3 nH. Hence, the package inductance L_p made the dominant contribution to the total parasitic inductance. The blocking capacitor C_1 is used to measure the voltage $V_r(t)$ across the thyristor during the turn-on process. The time resolution of the circuit with the load resistance $R_L = 50 \Omega$ was better than 0.5 ns.

Critical charge density

To determine the critical charge density the well known "dV/dt technique" was used. A forward dc voltage V_0 was applied to the thyristor. Then, an additional pulse of amplitude ΔV (rise time < 1 nsec) was applied. The 50 Ohm pulse generator TR 0306 with the rise time of 0.3 ns was used to form the dV/dt pulse. High frequency 50 Ohm circuit with the low parasitic inductance value (< 1.2 nH) was used to apply the pulse to the anode of the thyristor.

The minimum value of ΔV sufficient to turn on the thyristor was registered. The magnitude of the charge appearing in both bases of the thyristor Q_{cr} is equal to

$$Q_{cr} = \int_{V_0}^{V_0 + \Delta V_0} C_{jc}(V) \cdot dV$$

where C_{jc} is the capacitance of the central (collector) pn junction of the thyristor jc. The critical charge density n_{cr} was calculated according to the equation $n_{cr} = q_{cr}/e = Q_{cr}/(S \times W_1 \times e)$, where S is the thyristor area, W_1 is the thickness of the thin base, e is the electron charge.

The $C(V)$ dependence was measured at a frequency of 1 kHz in the range of forward voltage $0 < V_0 < V_b$ with an accuracy of 10^{-2} pF.

Forward current-voltage characteristics

Thyristors were turned-on using dV/dt effect at small anode current $I = 10-15$ mA. At time $t = 200$ ns after the turn-on, the pulse current I was passed through the turned-on thyristor. The pulse duration was equal to 200-500 ns. The voltage drop V on the structure at given current I was measured after time $t = 100$ ns from the beginning of the current pulse. As it was shown in [15], the steady state voltage drop on the 4H-SiC thyristor was achieved in about 50 ns. Hence the measured V values followed the steady state current-voltage characteristic.

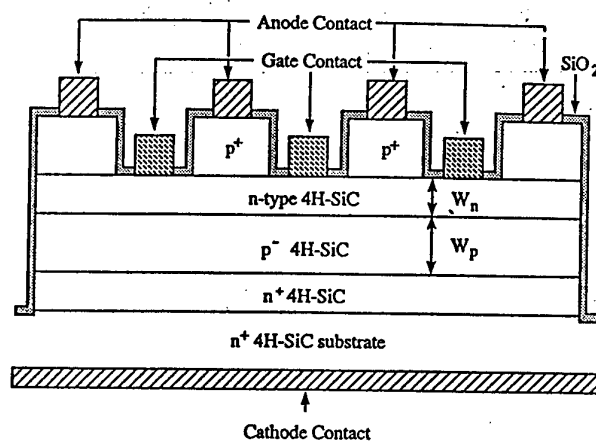


Fig. 1. Cross section of the n-p-n-p 4H-SiC thyristor

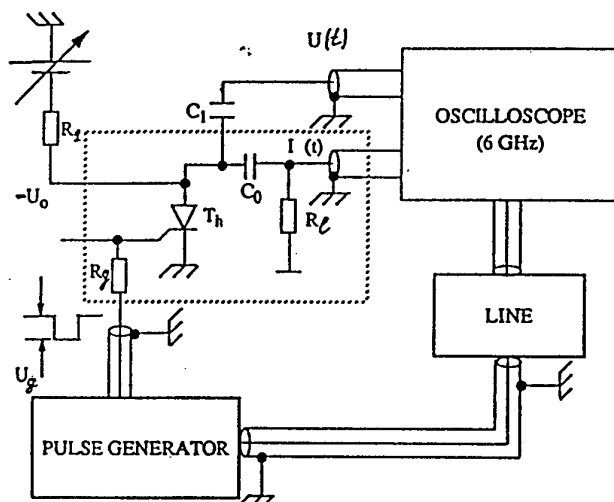


Fig. 2. Schematic diagram of the experimental setup for measuring of the turn-on characteristic.
 $C_1 = 20 \text{ nF}$, $R_f = 50 \Omega$

Turn-on spread

The thyristor structures investigated in this work are not designed specifically to study the spread of the on-state. However, one can estimate the j_0 value experimentally. Here j_0 is the critical current density at which the turned-on state does not spread and occupies only part of the structure.

If the anode current value I_a is high enough (> 15 mA), the on-state occupies all area of the structure. This can be judged from the recombination radiation [16, 17] which lies for SiC in visible part of wavelengths. The radiation can be observed easily through an optical microscope. In some thyristors, one can observe that a decreasing anode current localizes the on-state to a part of the structure. Light scattering into the substrate produces a luminous "halo" around the "on" parts of the structure. This halo allows one to judge qualitatively on the localization of the on-state. Knowing the anode current value and the area of the on-state S , one can find the j_0 value.

Frequency limitations

The frequency properties of the thyristors were investigated in a circuit of simple linear modulator (Fig 3.). In this circuit the capacitor C_0 is charged from an external bias source. The thyristor Th is switched-on by a gate pulse, following which C_0 discharges through the thyristor and the series resistor R_L . The linear modulator is the simplest circuit which allows comparing correctly the limiting work frequencies of different types of the thyristors [18].

4. RESULTS AND ANALYSIS

4.1. Turn-on process

The main results on the turn-on process investigations are described in paper [19] for 400 V thyristors and in papers [20, 21] for 700 V thyristors.

Typical time dependences of the voltage across the load resistance, $V_R(t)$, during turn-on process of 400 V structures are shown in Fig. 4 for different temperatures and for a forward blocking bias $V_O = 30$ V. The steady state current density j_0 , attained after the turn-on process terminates, is equal to $V_{RS}/R_L \cdot S = 1400$ A/cm², where V_{RS} is the steady state voltage drop across the load resistance R_L at the end of turn-on. At $j = 1.4 \cdot 10^3$ A/cm², V_{RS} depends only slightly on temperature, being equal to ~ 25.5 V over the whole temperature range $160 < T < 500$ K. Accordingly, the residual voltage drop across the thyristor structure V_n is equal to $V_O - V_{RS} = 4.5$ V for all temperatures. It can be seen from Fig. 4 that the turn-on process is strongly temperature dependent, especially at $T \leq 300$ K. The total turn-on time is about 180 nsec at 160 K and only about 10 nsec at 495 K.

The $V_R(t)$ dependences shown in a figure have a qualitatively usual form: a relatively fast exponential rise of current ($I = I_0 \exp(t/\tau_r)$), followed by slower part where the second derivative of current changes sign. The inset in Fig. 4 shows the temperature dependence of τ_r . It is seen that τ_r decreases monotonically with temperature increasing from $\tau_r = 63$ nsec at $T = 160$ K to $\tau_r = 1.9$ nsec at $T = 495$ nsec. It should be noted that such a strong temperature dependence of τ_r has been observed neither in Si nor in GaAs thyristors. It is unlikely that this dependence can be explained by a fall in life time of minority carriers in SiC with temperature decreasing [22]. As is well known, even a very strong several fold decrease of minority carrier life time has practically no reducing effect on τ_r [23]. In Ref. [15] it was noted that at 300 K τ_r is practically bias independent. The same situation was observed in the high temperature region $T > 300$ K. On the contrary, at low temperatures $T < 250$ K the dependence of τ_r on the bias V_O has a usual form: τ_r decreases monotonically with increasing bias. Fig. 5 shows the rise time constant τ_r as a function of bias V_O for the 400 V SiC thyristor under investigation at $T = 300$ K (curve 1) and $T = 220$ K (curve 2) and for comparably rated Si and GaAs thyristors with the same forward blocking voltage capability $V_{max} = 400$ V [24]. It is seen that the time constant τ_r for Si and GaAs thyristors decreases monotonically with increasing bias voltage. As far as we know such a dependence is observed for all types of Si and GaAs thyristors without any exception. The $\tau_r(V_O)$ dependence for SiC thyristors at $T = 220$ K is similar to these dependences. However, at $T > 300$ K τ_r is practically independent of V_O .

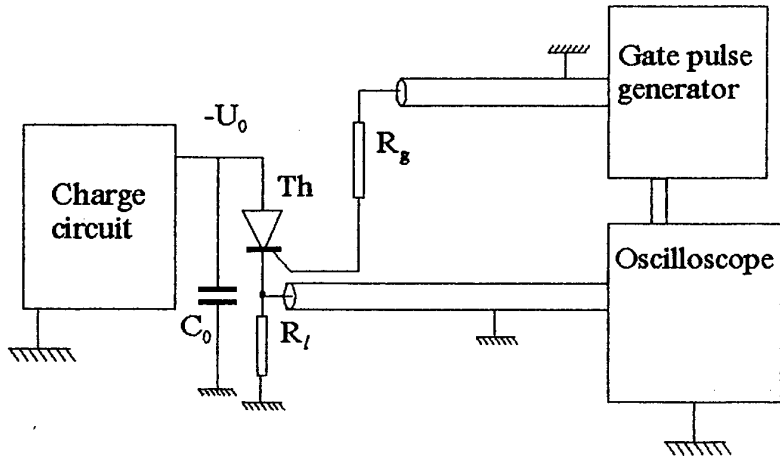


Fig. 3. Schematic experimental setup for measuring of frequency properties of 4H-SiC thyristors.
 $C_0 = 10 \text{ nF}$, $R_l = 1 \text{ Ohm}$ (ultra low-inductive resistor). The total pulse duration is about 100ns.

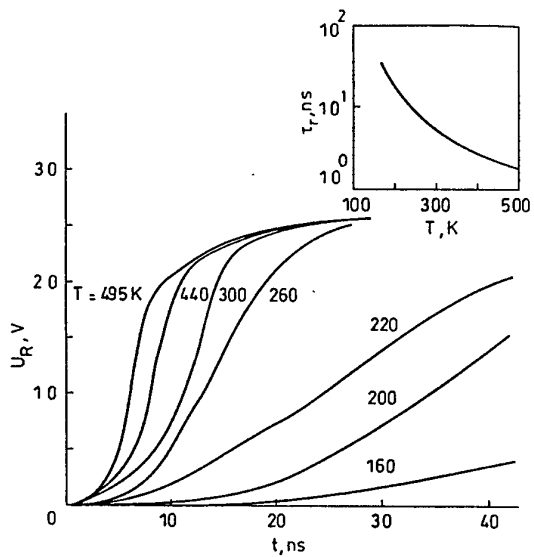


Fig.4. Time dependences of voltage across the load resistor $R_l = 50 \Omega$ during turn-on process at different temperatures. $V_O = 30 \text{ V}$.
 Inset: temperature dependence of the time constant of current rise τ_r .

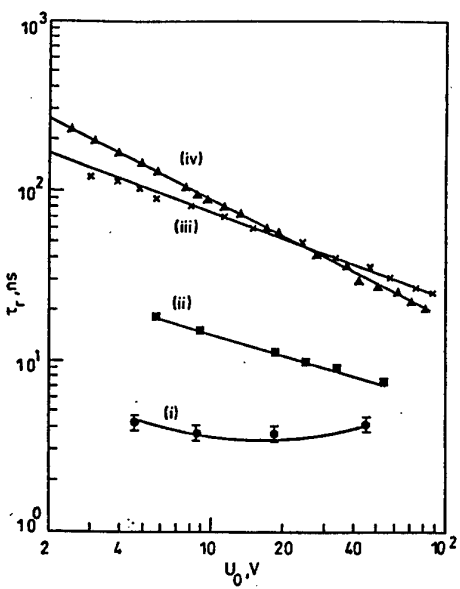


Fig. 5. Dependences of the current rise time constant t_r versus blocking voltage for various thyristor structures.

1,2 -400 V 4H-SiC thyristor (the structure under investigation). 1. T = 300 K 2. T - 220 K.
3 - Si thyristor, 4 - GaAs thyristor

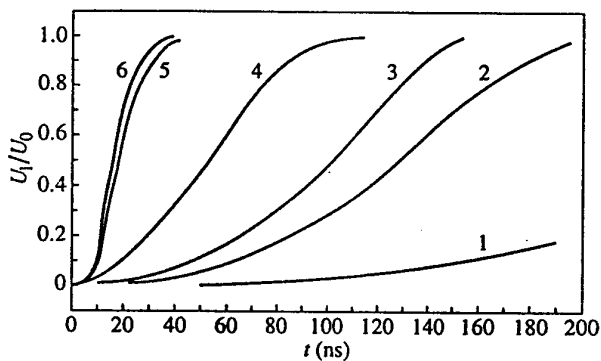


Fig.6. Time dependence of the voltage V_f during turn-on process on the series load resistance $R_L = 50 \Omega$ related to bias voltage V_0 .
T = 300 K. $V_0(V)$: 1 - 80, 2 - 100, 3 - 150, 4 - 180, 5 - 200, 6 - 450.

The absence of bias dependence of τ_r in 4H-SiC thyristors probably indicates that the turn-on mechanism in SiC thyristors is governed by diffusion, at least at $T > 300$ K. In the terms of diffusion mechanism of the turn-on process the time constant τ_r can be estimated by the following simplified expression:

$$\tau_r = (\vartheta_1 \cdot \vartheta_2)^{1/2}, \quad (1)$$

where $\vartheta_1 = W_1^2 / 2D_2$, $\vartheta_2 = W_1^2 / 2D_1$. The subscript "2" refers to the voltage supporting base, subscript "1" to the thin high doped base; D is the diffusion constant. For SiC thyristors under investigation, with the electron diffusion constant assumed to be $10 \text{ cm}^2/\text{sec}$ at 300 K for p-base and the hole diffusion constant to be equal $1.5 \text{ cm}^2/\text{sec}$ for the highly doped n-base, the τ_r is estimated to be 3 nsec . It is seen (curve 1, Fig.5) that at room temperature there is a very reasonable agreement between the experimental results and an estimation made according to Eq(1). However, as temperature becomes higher the mobility and the diffusion coefficient decrease both in p- and n-SiC base layers. According to Eq(1), τ_r can be expected to increase with increasing temperature. Meanwhile, experiment shows that, on the contrary, τ_r decreases as temperature is elevated (from about 4 nsec at 300 K to 1.9 nsec at 495 K). Further analysis is necessary for establishing the reason for this unusual behavior of SiC thyristors.

Fig.6. shows the time dependences of V/V_0 at 300 K for different values of the bias voltage V_0 during turn-on process of 700 V thyristor structures [20]. Here V_0 is the voltage on the series load resistance $R_s = 50 \Omega$. At the end of the turn-on process the steady state current density j_0 is equal approximately $j_0 = V_0/R_s$. Hence $j_0 = 1.5 \cdot 10^3 \text{ A/cm}^2$ at $V_0 = 450 \text{ V}$ (curve 6, Fig.6) and $j_0 = 270 \text{ A/cm}^2$ at $V_0 = 80 \text{ V}$ (curve 1, Fig.6). It can be seen from Fig.6 that current rise time decreases sharply with bias increasing at $V_0 \leq 200 \text{ V}$. On the contrary, at $V_0 \geq 200 \text{ V}$ both total time of the current rise and current rise time constant τ_r are practically independent of bias V_0 .

It should be noted that the $\tau_r(V_0)$ dependences for these thyristors differ qualitatively from the $\tau_r(V_0)$ dependences for the relatively low-voltage 400 V 4H-SiC thyristors. As one can see, in thin-base, low-voltage SiC thyristors $\tau_r = 3 \text{ nsec}$ and it does not depend on bias V_0 over the whole range of V_0 from $V_0 = 5 \text{ V}$ to $V_0 = 150 \text{ V}$. On the contrary, strong dependence of τ_r on V_0 for 700 V thyristors demonstrates very clear the contribution of the field mechanism into the turn-on process .

Fig.7 shows the V_0 dependence for different temperatures at $V_0 = 200 \text{ V}$ for 700 V thyristor. It can be seen from the figure that both total current rise time and τ_r decrease monotonically with temperature increasing. At $T = 500 \text{ K}$ (curve 5, Fig.7) $\tau_r = 1.2 \text{ nsec}$. As far as we know this is the minimal value of τ_r observed for SiC thyristors. As it was mentioned above, the strong bias dependence of τ_r demonstrates that the turn-on mechanism in 700 V SiC thyristors is dominated by field process. Hence, one could expect that τ_r will increase with temperature increasing because either mobility of carriers or diffusion coefficient decrease monotonically with temperature enhancement over the whole temperature range $300 \text{ K} - 500 \text{ K}$. However the opposite situation was observed experimentally as well as for 400 V thyristors (Fig. 7). Hence, it is necessary to perform further analysis for establishing the reason of this unusual temperature dependence of τ_r in 4H-SiC thyristors.

4.2. Critical charge density

At $T > 550\text{K}$ and forward voltage $V_0 > 5\text{V}$, the dV/dt switching in 4H-SiC thyristors is qualitatively analogous to the dV/dt effect in Si and GaAs thyristors. The curve (1) in Fig. 8a shows the dependence of the critical charge density n_{cr} versus forward voltage V_0 . Curve (2) shows the $n_{cr}(V_0)$ dependence for GaAs thyristor with approximately the same breakdown voltage V_b [25]. The critical charge value for the SiC thyristor is rather small $Q_{cr} = 5.2 \text{ pC}$ at $V_0 = 5\text{V}$ and $Q_{cr} = 0.32 \text{ pC}$ for $V_0 = 100 \text{ V}$. However, due to small n-base thickness ($W_n = 0.55 \mu\text{m}$) and very small thyristor area ($S = 3.6 \cdot 10^{-4} \text{ cm}^2$), the critical charge density is sufficiently high: $n_{cr} = 1.5 \cdot 10^{15} \text{ cm}^{-3}$ at $V_0 = 5\text{V}$ and $n_{cr} = 10^{14} \text{ cm}^{-3}$ at $V_0 = 100 \text{ V}$.

At $T < 450 \text{ K}$ the dV/dt effect has been found to be anomalous within the whole range of the V_0 values for a SiC thyristors. One can see this easily by comparing the $\Delta V(V_0)$ dependencies for SiC (Fig. 9a) and Si

(Fig.9b) thyristors. The usual dV/dt effect is characterized by an "infinitely long" current pulse. That is, the exponential increase of the anode current begins before the end of the dV/dt pulse. It is possible to

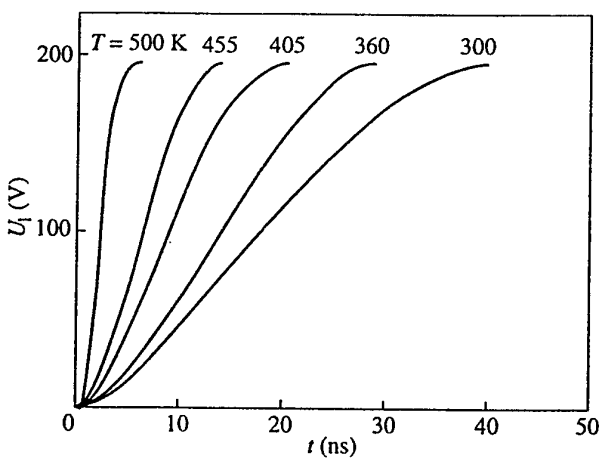


Fig. 7 Time dependence of V_i for different temperatures at $V_0 = 200$ V. $R_i = 50 \Omega$. T(K) : 1 - 300, 2 - 360, 3 - 405, 4 - 455, 5 - 500.

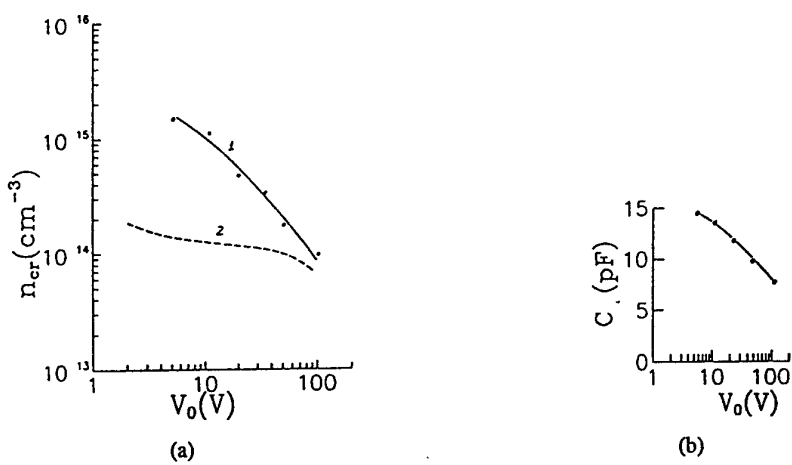
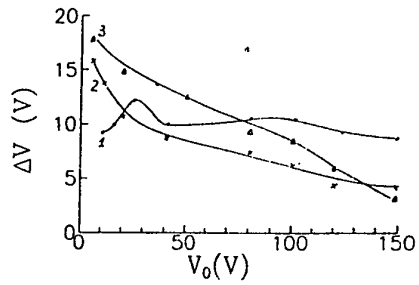
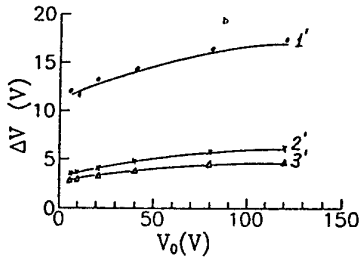


Fig. 8. (a) the dependencies of the critical charge density n_{cr} versus forward voltage V_0 . 1 - 400 V 4H-SiC thyristor, 560 K 2 - GaAs thyristor, 300K. (b) The dependence of the central (collector) pn junction capacitance C_{jc} versus forward voltage V_0 for 4H-SiC thyristor, 560K.



(a)



(b)

Fig. 9. (a) The dependencies of the pulse amplitude ΔV turned-on the 4H-SiCthyristor by the dV/dt effect versus forward voltage V_0 at 300K. The pulse duration (nsec): 1 - 20, 2 - 130, 3 - 400.

b) The same dependencies for commercial Si thyristor KU-103, 300K The pulse duration (nsec): 1' - 20, 2' - 130, 3' - 400.

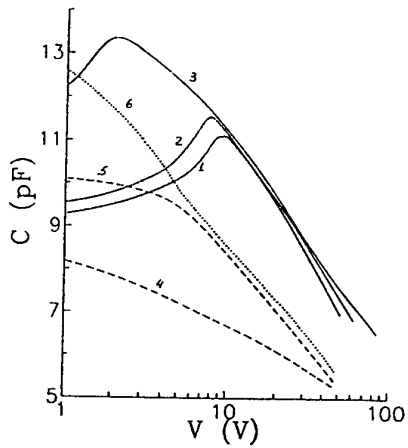


Fig. 10 Capacitance - voltage dependencies measured between gate and cathode electrodes.
1-3 forward voltage, T(K): 1 - 300, 2 - 390, 3 - 560. 4-5 reverse voltage, T(K): 4 - 300, 5 - 390.
6 forward voltage for Si thyristor KU-103, T=300 K.

turn-on the thyristor by a shorter pulse duration, but that requires a correspondingly larger pulse ΔV . It can be seen from the Fig. 9b that for a Si thyristor, a smaller pulse duration requires a larger ΔV magnitude in the whole range of dc voltage value V_0 . This kind of $\Delta V(t)$ dependencies is typical for all Si and GaAs thyristors at any temperatures. One can see in Fig. 9a that the opposite is true for SiC thyristor. At $V_0 < 20$ V, a smaller pulse duration requires a smaller ΔV magnitude to turn on the thyristor. To appreciate better this very unusual situation, let us imagine for example that at $V_0 = 10$ V, a dV/dt pulse is applied to the thyristor. The magnitude of the pulse ΔV is large enough to turn-on the thyristor at $t = 20$ nsec. However, if the pulse is not interrupted after 20 nsec, the thyristor is not turned on. Hence the applied pulse impedes the turn on process. Only at $V_0 > 140$ V, the $\Delta V(t)$ dependence takes the usual form (compare with the Fig. 9b).

Investigations show that two effects take part for this phenomenon. First, at $T < 450$ K and $V_0 = 0$, the capacitance of the collector p-n junction C_{jc} is sufficiently larger than the capacitance of the emitter junction C_{je2} . A high C_{jc}/C_{je2} ratio does not occur commonly in Si and GaAs thyristors. It will be shown that at $C_{jc} > C_{je2}$, the turn on process by dV/dt effect changes qualitatively. It can even be said that the term "dV/dt effect" is invalid at $C_{jc} \gg C_{je2}$. Secondly, the spectrum of the deep levels near j_c junction is essentially different from the spectrum of the deep levels near j_{e2} junction. This follows directly from the temperature dependence of the dV/dt effect.

In Fig. 10 several curves displaying the dependence of the capacitance

$$C = \left[\frac{1}{C_{jc}} + \frac{1}{C_{je2}} \right]^{-1} \quad (2)$$

versus bias voltage are shown. The voltage bias was applied between the gate and cathode contacts. For curves 1-3, the polarity of the voltage corresponds to the reverse bias on the jc junction and to the forward bias on the j_{e2} junction (forward bias on the thyristor). Dashed lines 4, 5 represent the $C(V)$ dependencies for another polarity of voltage between the gate and cathode contact. Dotted curve 6 in Fig. 10 represents the $C(V)$ dependence for commercial Si thyristor KU-103 (forward bias).

In Si and GaAs thyristors, the doping level of the thick base is usually the same near both junctions. In this case, $C_{jc} = C_{je2}$ at $V_0=0$. As forward bias is applied, C_{jc} decreases and C_{je2} increases. Even at $V_0 > 3-4$ V_{bi} (V_{bi} is the built in potential), the condition $C_{jc} \ll C_{je2}$ is fulfilled and C value is practically equal to C_{jc} (Eq. 2). For Si thyristors the condition $C_{jc} \ll C_{je2}$ is valid if $V_0 > 2-3$ V; and for GaAs thyristors - if $V_0 > 3-4$ V. However, if $C_{jc} > C_{je2}$ at $V_0=0$, the other situation is realized. A major part of the bias applied falls on the junction j_{e2} . The capacitance C_{je2} increases with an increase in forward voltage as C_{jc} value is practically constant. At $C_{jc} > C_{je2}$. As a result, C value increases with an increase in anode bias (curves 1-3 in Fig. 10) A large enough bias results in the condition $C_{jc} = C_{je2}$. A further increase in the bias leads to a decrease in the total capacitance C . A similar relation has been observed for SiC thyristors at forward bias (curves 1-3). At reverse bias, $C(V)$ dependencies have the usual form (compare curves 4 and 5 with curve 6). One can see from Fig. 10 that j_c and j_{e2} junctions are characterized not only by the different capacitance values at $V_0=0$, but also by the different temperature dependencies of the capacitance. This directly proves a different spectrum of the deep levels near the junctions.

The dV/dt pulse applied is divided between j_{e1} , j_c and j_{e2} junctions. Because $C_{je1} \gg C_{jc}$, C_{je2} , the voltage drop on C_{je1} can be neglected. Having $C_{jc} = C_{je2}$ at $V_0=0$ as it is usually realized for Si and GaAs thyristors, the dV/dt pulse is almost completely applied to the central j_c junction, provided $\Delta V > 3-4$ V. Majority carriers are displaced into the thyristor bases by the expanded space charge region of the central j_c junction. These excess majority carriers initiate the injection of minority carriers from emitter p-n junctions. In this way, the usual dV/dt mechanism is realized. As can be seen from Fig. 9, at $C_{jc} > C_{je2}$, the essential different mechanism of the turn on is realized in 4H-SiC thyristor provided $T < 450$ K. Further analysis is necessary for establishing the reason for this unusual behavior of SiC thyristors which is very important from practical point of view.

4.3. Forward current-voltage characteristics

Forward current-voltage characteristics of 400 V and 700 V devices were studied in the papers [14, 15, 26, 27]. For 400 V structures I-V characteristics were studied up to current density $j \geq 10^5 \text{ A/cm}^2$. For 700 V structures I-V characteristics were studied up to current density $j \geq 6 \times 10^4 \text{ A/cm}^2$.

In Fig.11 curve 1 shows the dependence of current density $j = I/S$ versus residual voltage drop V at 300K for 400 V thyristor. Current - voltage characteristics has an usual form: differential resistance $R_d = dV/dj$ decreases monotonically with bias increase. In inset curve 1' shows the current - voltage characteristic of the same 4H-SiC thyristor structure at super high current density (up to $7 \times 10^4 \text{ A/cm}^2$). One can see that in the current density range $10^4 - 7 \times 10^4 \text{ A/cm}^2$ the current - voltage characteristic has a form of a straight line. If one supposes that the contact resistance r makes the main contribution to differential resistance R_d at high current density, the value $r = R_d/2 = 1.5 \times 10^{-4} \text{ Ohm} \times \text{cm}^2$ looks quite reasonable [28].

Curve 2 in Fig.11 shows the current - voltage characteristic of the same structure at $T = 600 \text{ K}$. Curves 3 and 4 in Fig.11 show the current - voltage characteristics of rated GaAs (curve 3) and Si (curve 4) thyristors with approximately the same blocking voltage $V = 350-400 \text{ V}$. It is seen that at $j > 2 \text{ kA/cm}^2$ the voltage drop on the rated GaAs and Si thyristors is essentially greater than on the SiC thyristor. It would be expected as to block the same voltage the rated Si and GaAs thyristors have more wide and lower doped bases. Besides, the achievement of the steady state voltage drop took much more time for these thyristors (especially for Si one) than for SiC thyristor [14,15]. Hence one can expect that SiC thyristors may be not only high temperature and radiation hardness switches; they may provide more high efficiency than rated Si and GaAs thyristors at high and super high current densities.

To compare correctly the calculated and experimental characteristics, the lifetimes of minority carriers τ_n and contact resistivity R_c have been measured for the structures of both types: 400 V and 700 V. The τ_n was equal 80ns at $T = 300\text{K}$, and $\tau_n \approx 280\text{ns}$ at $T = 500\text{K}$. The W/L ratios estimated from the measured τ_n values agree reasonable with the values and temperature dependencies of the critical charge densities measured in these structures earlier [29]. (W is the width of the blocking p-base, L is the ambipolar diffusion length). The R_c falls within the range of $(1.5 - 4) \times 10^{-4} \Omega \text{ cm}^2$ and practically temperature independent. Forward current-voltage characteristics have been calculated for the thyristors with the breakdown voltages of 400V and 700V in the temperature range of 300 - 500K up to current densities $\geq 10^4 \text{ A/cm}^2$. The calculations were made in the frame of the theory which takes into account the decrease of the emitter injection coefficient at high current densities [30]. Calculated and experimental results agree well within the wide range of current densities and temperatures (Fig. 12)

Fitting parameter of the theory is the saturation leakage current density j_s . The values of j_s were defined for SiC p-n junction for the first time: $j_s \approx 10^{-46} - 10^{-45} \text{ A/cm}^2$ at 300K, $j_s \approx 10^{-22} - 10^{-23} \text{ A/cm}^2$ at 500K, and $j_s \approx 10^{-18} - 10^{-17} \text{ A/cm}^2$ at 600K (at 300 K the values of j_s for Si p-n junctions falls in the range of $j_s \approx 10^{-14} - 10^{-12} \text{ A/cm}^2$, for GaAs p-n junctions- in the range of $10^{-18} - 10^{-16} \text{ A/cm}^2$).

In the frame of such calculations, the related contributions of contact resistivity and non-ideality of the emitter junctions to the voltage drop on the thyristor structures may be considered (Fig. 13). It is seen in Fig. 13, that even with the same quality of junctions , the voltage drop may be reduced essentially (Curve 2). "Ideal" junctions (Curve 3) may be practically considered as a very high doped emitter layer with the high enough values of τ_n and diffusion coefficient D_p . One can see that the combination of such an "ideal" p-n junction and contacts with low resistance may provide the voltage drop values across the SiC p-n junctions at high current densities which is sufficiently less than across identically rated Si and GaAs thyristors.

4.4. Turn-on spread

It is well known that for every thyristor structure, there exists a critical current density j_0 at which the turned-on state does not spread and occupies only part of the structure. Under this condition, the critical density of minority carrier charge in the thin base of the thyristor is equal to $n_0 = 2 n_{cr}$ [12]. For GaAs and Si thyristors, the relationship between j_0 and n_{cr} has been investigated in [16]. The value of j_0 can be estimated using the simplest model of the thyristor [12, 31]. It is assumed that in the turned-on state the minority carrier concentration n_0 is constant along the thyristor bases. For this case,

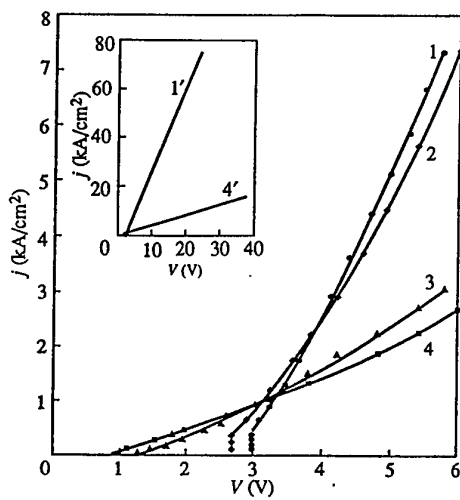


Fig.11. Current-voltage characteristics of 400 V SiC (curves 1 and 2), GaAs (curve 3) and Si (curve 4) thyristors with the same maximal blocking voltage V . Curves 1,3,4 - $T = 300\text{ K}$, curve 2 - $T = 600\text{ K}$. Inset shows the current-voltage characteristics of SiC (curve 1') and Si (curve 4') thyristors at super high current densities. $T = 300\text{ K}$.

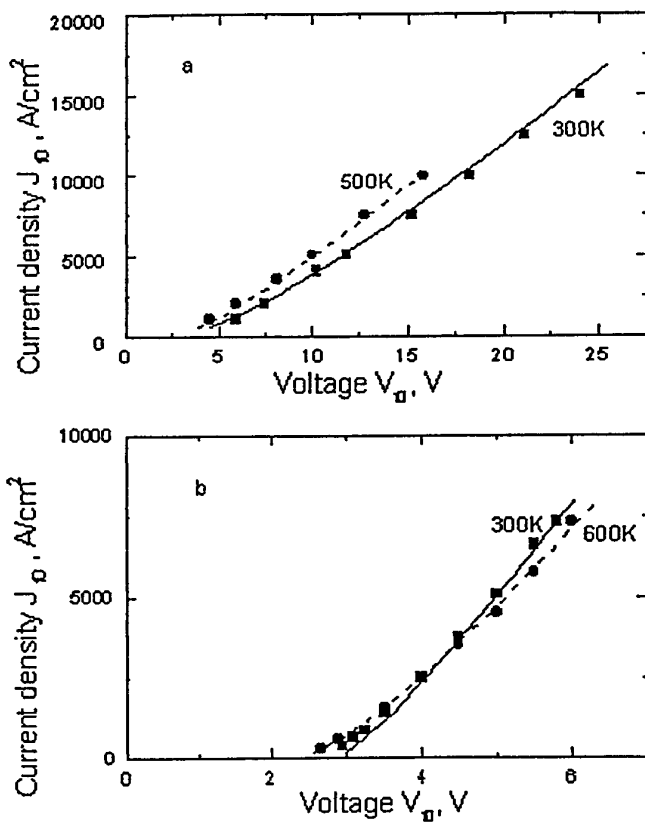


Fig. 12. The current-voltage characteristics of the thyristor structures. Curves are calculated dependencies; marks represent the related experimental data.

a. 700 V thyristor $T=300\text{K}$: $R_c = 4 \cdot 10^{-4} \Omega \cdot \text{cm}^2$, $\tau_n = 80\text{ns}$, $j_s = 1.1 \cdot 10^{-45} \text{ A/cm}^2$

$T=500\text{K}$: $R_c = 4 \cdot 10^{-4} \Omega \cdot \text{cm}^2$, $\tau_n = 280\text{ns}$, $j_s = 1.5 \cdot 10^{-23} \text{ A/cm}^2$

b. 400V thyristor $T=300\text{K}$: $R_c = 1.5 \cdot 10^{-4} \Omega \cdot \text{cm}^2$, $\tau_n = 80\text{ns}$, $j_s = 1.5 \cdot 10^{-46} \text{ A/cm}^2$

$T=600\text{K}$: $R_c = 1.5 \cdot 10^{-4} \Omega \cdot \text{cm}^2$, $\tau_n = 280\text{ns}$, $j_s = 4 \cdot 10^{-18} \text{ A/cm}^2$

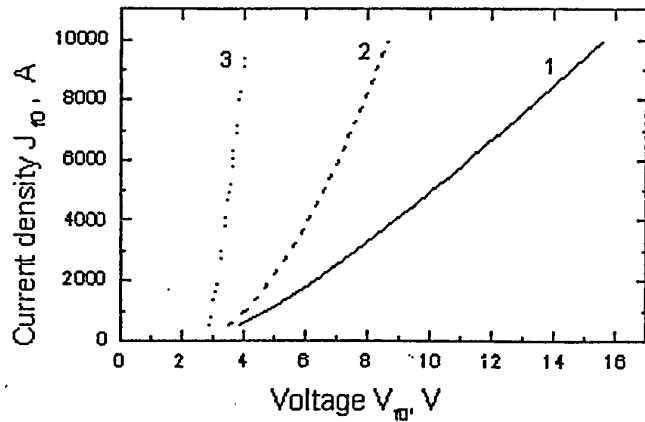


Fig 13. Calculated current-voltage characteristics of 700 thyristor.

1. Current-voltage characteristic reproduces solid curve of Fig. 12a.
2. Calculation for the same set of the parameters but with $2R_c = 10^4 \Omega \cdot \text{cm}^2$ (instead of $2R_c = 8 \cdot 10^4 \Omega \cdot \text{cm}^2$ as it has been taken for the curve 1).
3. Calculation for the case of $2R_c = 10^4 \Omega \cdot \text{cm}^2$ and "ideal" junctions ($j_s = 0$).

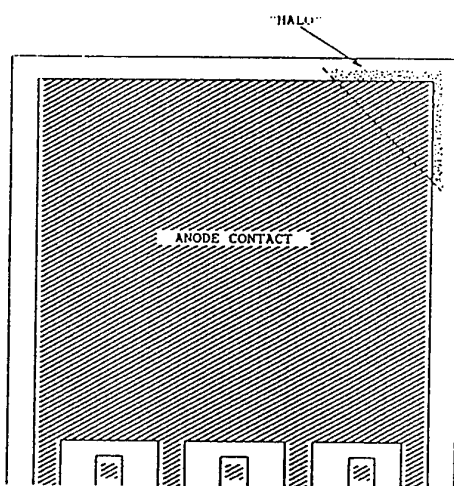


Fig. 14. On-state in 4H-SiC thyristor at anode current $I_a = 3.8 \text{ mA}$

$$j_0 \equiv e \cdot n_0 \cdot \left[\frac{W_n}{\tau_p} + \frac{W_p}{\tau_n} \right] \approx 2e \cdot n_0 \cdot \left[\frac{W_n}{\tau_p} + \frac{W_p}{\tau_n} \right] \quad (3)$$

For thin n-base of the thyristor, one can assume that the common-base current gain α is equal to 0.8.. Using the usual expression for the common base circuit configuration gain, it is easy to obtain the hole lifetime in the thin base of the thyristor: $\tau_p = 3.8 \cdot 10^{-9}$ s. The diffusion coefficient $D_p = 2 \text{ cm}^2/\text{s}$ has been taken for this calculation. To estimate the electron lifetime in the wide thyristor base τ_n one can assume the usual relation between wide base width W_p and electron diffusion length L_n : $W_p/L_n = 3$. Using the electron diffusion coefficient $D_n = 15 \text{ cm}^2/\text{s}$, a τ_n of $1.5 \cdot 10^{-9}$ s was derived. Taking a value of n_{cr} to be $2 \cdot 10^{15} \text{ cm}^{-3}$, we obtain a j_0 value of $2 \cdot 10^2 \text{ A/cm}^2$.

The thyristor structures investigated in this paper are not designed specifically to study the spread of the on-state. However, one can estimate the j_0 value experimentally. If the anode current value I_a is high enough ($> 15 \text{ mA}$), the on-state occupies all area of the structure. This can be judged from the recombination radiation which lies for SiC in visible part of wavelengths. The radiation can be observed easily through an optical microscope. Light scattering into the substrate produces a luminous "halo" around the "on" parts of the structure. This halo allows one to judge qualitatively on the localization of the on-state. In some thyristors, one can observe that a decreasing anode current localizes the on-state to a part of the structure (see Fig. 14).

In Fig. 14, the boundaries of the luminous halo are shown at the anode current I_a of 3.8 mA . Since it is difficult to observe the on-state distribution under the opaque anode electrode, it was assumed that the boundary of the on-state under the electrode is a straight line (dashed line in Fig. 14). Knowing the anode current value and the area of the on-state S , one can find the j_0 value. The experimental values of j_0 fall in the range of $3 \cdot 10^2 \text{ A/cm}^2$ and $7.5 \cdot 10^2 \text{ A/cm}^2$. Taking into account the qualitative character of the theoretical model an agreement between theoretical and experimental estimations are quite satisfactory.

4.5 Frequency limitations

Frequency properties of 4H-SiC thyristors with a forward blocking voltage $V_b \sim 400 \text{ V}$ and $V_b \sim 700 \text{ V}$ have been investigated up to current densities $j \geq 14000 \text{ A/cm}^2$ with operating frequency of 500 KHz for 400 V structures and up to $j \geq 750 \text{ A/cm}^2$ with operating switching frequency of 500 KHz for 700 V structures [32]. The results obtained for SiC thyristors were compared with the related data for one of the fastest Si industrial thyristors KU221 with a blocking voltage of 400-600 V and a limiting operating frequency of about 30 kHz. (The p-n-p-n thyristor KU221 had the voltage blocking n-layer of $120 \mu\text{m}$ thick with donor concentration $N_d - N_a = 1.4 \cdot 10^{14} \text{ cm}^{-3}$. The effective pulse active area of the device with pulse duration of about 100 ns was equal $S = 6.3 \cdot 10^{-3} \text{ cm}^2$).

Experimental results obtained are shown in Fig. 15 where they are compared with the related data for Si thyristor KU221 and the theoretical estimation of limiting operating frequency for 400 V thyristors. The highest operation frequency achieved for 400 V thyristor is equal to about 1000 kHz (at current density $j \geq 2700 \text{ A/cm}^2$) At $j \geq 14000 \text{ A/cm}^2$ the highest operation frequency is equal to 500 kHz. For rated Si thyristor the highest operation frequencies are equal to 30 kHz at $j=1500 \text{ A/cm}^2$ and 5 kHz at $j=10^4 \text{ A/cm}^2$. It is seen that at the same current density, the operating frequency of SiC thyristors is approximately two orders higher than that for the identically rated Si thyristor.

In the simple circuit of linear modulator, the limiting operating frequency f_0 is basically determined by switch-off time τ_s (τ_s is the recovery time of the blocking ability). In the linear modulator circuit τ_s value and the minority carrier lifetime in the voltage-blocking base, τ , are related by:

$$\tau_s = \tau \cdot \ln \left(\frac{j}{j_0} \right) \quad (4)$$

where j is the forward current density in on-state and j_0 is the parameter of the theory [7].

The dependence of τ_s on j for 4H-SiC thyristors was measured in paper [27]. The slope of this dependence defines the minority carrier lifetime in the voltage-blocking base, τ , and the forward current density j at $\tau_s = \tau$ defines j_0 . It is easy to establish from this dependence that τ and j_0 are equal to about $\approx 80 \text{ ns}$ and

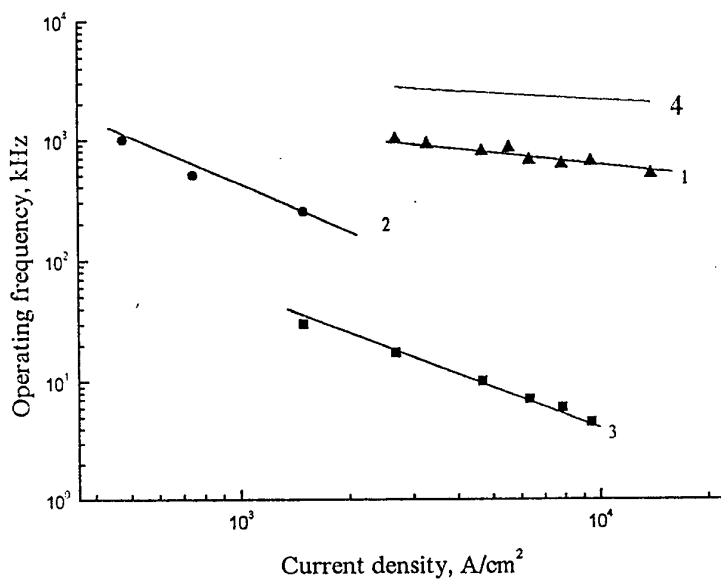


Fig. 15. Dependence of limiting operating frequency on current density.
 1- 400V SiC thyristor, 2 - 700V SiC thyristor, 3 - Si thyristor KU221 with blocking voltage of 400 -600 V.
 4 - Theoretical estimation of limiting operating frequency (Eq.(4)) for 400V 4H-SiC thyristor.

≈ 30 A/cm² respectfully. Taking limiting operating frequency $f_0 = 1/\tau_r$ one can calculate the f_0 on j dependence (Curve 4 in Fig. 15). It is seen that the slopes of the theoretical and experimental dependences are very close. It is seen, the theoretical estimation for the limiting frequency f_0 is several times higher than the experimentally achieved values.

Another way to estimate the f_0 for SiC thyristors is the following. Comparing thyristor structures produced from the different semiconductor materials one can check that the thickness of the voltage-blocking base W must be inversely proportional to E_i : $W \sim 1/E_i$. To keep the same level of the base modulation, the W/L ratio should be kept the same. Here $L = \sqrt{D_a \tau_r}$ is the diffusion length and D_a is the ambipolar diffusion coefficient,

$$D_a = \frac{\mu_p \cdot p \cdot D_n + \mu_n \cdot n \cdot D_p}{\mu_n \cdot n + \mu_p \cdot p} \quad (5)$$

p , n , D_p , D_n , and μ_p , μ_n are the concentrations, diffusion coefficients, and mobilities of holes and electrons respectively. It is easy to see that the D_a values are rather close for Si and 4H-SiC at high injection levels ($n \approx p$), assuming $\mu_p \approx 10^2$ cm²/Vs and $\mu_n \approx 10^3$ cm²/Vs for 4H-SiC. Hence, the τ value must be inversely proportional to E_i^2 : $\tau_r \sim 1/E_i^2$. As mentioned above, the breakdown electric field E_i in SiC is an order of magnitude higher than E_i in Si. For Si, $E_i \approx 4 \cdot 10^5$ V/cm at $N = 3 \cdot 10^{16}$ cm⁻³; for SiC, $E_i \approx 4 \cdot 10^6$ V/cm at $N = 3 \cdot 10^{16}$ cm⁻³. This means that the theoretical limiting frequency for SiC thyristors must be two orders higher than that for the Si thyristors with the same blocking voltage. Taking $f_0 \approx 30$ kHz for Si thyristor, one can expect $f_0 \approx 3000$ kHz for identically rated 4H-SiC thyristor at equal current densities. It is seen that both theoretical estimations give very close results.

Experiments show that the main obstacle to increase the frequency f_0 is the self-heating of the devices. Indeed, the temperature rise makes τ_r higher and j_0 lower: at $T = 500$ K for 400 V thyristors $\tau_r \approx 280$ ns and $j_0 \approx 0.7$ A/cm². Both these effects make longer τ_r (see Eq. (4) and, accordingly, reduce f_0 . Besides, reducing j_0 means that the critical switch-on charge n_{cr} decreases accordingly ($n_{cr} \sim j_0$). As a result, the maximum voltage ramp (dV/dt) also falls. Hence a thyristor structure with the optimal design for 300 K, has too large τ_r , and too small j_0 and n_{cr} at elevated temperatures. From this follows that one of effective ways to increase the limiting operating frequency f_0 is to reduce τ_r at room temperature so that the optimal τ_r values can be reached at higher temperatures.

5 CONCLUSIONS AND RECOMMENDATIONS

As a result of this work all main parameters of SiC thyristors are established.

It is shown that for 400 V thyristors the current rise time constant τ_r can be as small as 1.9 ns (at $T = 500$ K). For 700 V 4H-SiC thyristor minimal value of τ_r is equal $\tau_r = 1.2$ nsec. (at $T \geq 500$ K). As far as we know these are the minimal values of τ_r observed for SiC thyristors. They are comparable to the best results for highly optimized Si thyristors. The strong bias dependence of τ_r demonstrates that the turn-on mechanism in 4H-SiC at elevated temperatures is dominated by field process.

The critical charge density n_{cr} was measured for the first time in SiC thyristors. The value of n_{cr} was found to be sufficiently high: $n_{cr} = 1.5 \cdot 10^{15}$ cm⁻³ at $V^0 = 5$ V and $n_{cr} = 10^{14}$ cm⁻³ at $V^0 = 100$ V. It was mentioned that the structures optimized at 300 K has too large τ_r , and too small n_{cr} at elevated temperatures.

Forward current-voltage characteristics of 400 V and 700 V devices were studied for 400 V structures up to current density $j \geq 10^5$ A/cm². For 700 V structures I-V characteristics were studied up to current density $j \geq 6 \cdot 10^4$ A/cm². It was shown experimentally for the first time that SiC thyristors may be not only high temperature and radiation hardness switches; they may provide more high efficiency than rated Si and GaAs thyristors at high and super high current densities.

Critical current density j_0 at which the turned-on state does not spread and occupies only part of the structure was measured in SiC thyristors for the first time and compared with theoretical estimations. Measured j_0 values fall in the range of $3 \cdot 10^2$ A/cm² and $7.5 \cdot 10^2$ A/cm². These values are comparable to critical current density in power Si thyristor structures.

Frequency properties of 4H-SiC thyristors have been investigated up to current densities $j \geq 14000 \text{ A/cm}^2$ with operating frequency of 500 KHz for 400 V structures and up to $j \geq 750 \text{ A/cm}^2$ with operating switching frequency of 500 KHz for 700 V structures. It is shown that at the same current density, the operating frequency of SiC thyristors is approximately two orders higher than that for the identically rated Si thyristor.

It seems that the most important problem for SiC thyristors now is the optimization of the structures taking into account the temperature dependences of free carrier concentrations in the bases of the thyristors, real spectrum of deep levels in n- and p- bases, and current density dependence of current gain coefficients of n-p-p and p-n-p transistor sections. As a result of this optimization, one can hope to design SiC thyristors with extremely low switch-on time, very small residual forward voltage at high and super high current density, and extremely high operation frequencies.

The results obtained in the course of this work were published in Refs. [19-21,26,27,32].

19. N.V. Dyakonova, M.E. Levenshtein, J.W. Palmour, S.L. Rumyantsev, and R. Singh. 4 Intern. Symp. on Semicond. Device Research. (ISDRS-97), Charlottesville, USA, Dec. 10-13, 1997, pp.367-370.
20. N.V. Dyakonova, M.E. Levenshtein, J.W. Palmour, S.L. Rumyantsev, and R. Singh Semicond. Sci. Technol. v.13, no 2, pp. 241-243, (1998).
21. N.V. Dyakonova, M.E. Levenshtein, J.W. Palmour, S.L. Rumyantsev, and R. Singh, MRS Spring Meeting 1998, April 13-17, San Francisco, F5.1, p. 113
26. M.E. Levenshtein, J.W. Palmour, S.L. Rumyantsev, and G.S. Singh, Abstracts of 2nd European Conference on Silicon Carbide and Related Materials. Montpellier, France, Sept. 02-06, 1998, pp. 231-232
27. M.E. Levenshtein, J.W. Palmour, S.L. Rumyantsev, and R. Singh, Semicond. Sci. Technol. v. 13, p. 1006 (1998)
32. M.E. Levenshtein, J.W. Palmour, S.L. Rumyantsev and R. Singh, Submitted in: Semicond. Sci. Technol. September 1998.

Literature Cited

1. Palmour J W, Allen S T, and Waltz D G 1995 Techn. Digest of Int. Conf. on SiC and Related Mater., ICSRM-95, Kyoto, Japan, pp.319-320.
2. Andreev A N, Strel'chuk A M, Savkina N S, Snegov F M, and Chelnokov V E., Semiconductors **29**, 561, (1995)
3. V.A.Dmitriev, S.N.Vainshtein, M.E.Levinshtein, V.E.Chelnokov, Electron.Lett., vol.**24**, p.1032, (1988).
4. J.A.Edmond, J.W.Palmour, C.H.Carter, Proc. of Intern.Semicond.Dev. Research Symp. ISDRS-91, Charlottesville, Dec.4-6, 1991, p.487.
5. J.W.Palmour, J.A.Edmond, H.S.Kong, C.H.Carter,Jr., Silicon Carbide and Related Materials, Ins. of Phys. Conf.Ser., vol.137, p.499.
6. J.W.Palmour, S.T.Allen, D.G.Waltz, Techn. Digest of Int. Conf. on SiC and Related Materials, ICSRM-95, Kyoto,Japan, 1995, p.319.
7. K. Xie, J.H. Zhao, J.R. Flemish, T. Burke, W.R. Buchwald, G.Lorenzo and H.Singh IEEE Electron Device Letters, v.17(3), p.142-144 (1996)
8. K. Weiser, R. S. Levit, M. I. Nathan, G. Burns, J. Woodall, Trans. AMIE, p. 230, 1964.
9. A. I. Uvarov. Critical Turn-on Charge of a Thyristor. in: Physics of p-n junctions and semiconductor devices. Ed. by S.M.Ryvkin and Yu.V.Shmartsev, Consultants Bureau -New York-London, 1971. p.170
10. A. I. Uvarov. Conditions for Turning on a Thyristor by Short Gate Current Pulses. in: Physics of p-n junctions and semiconductor devices. Ed. by S.M.Ryvkin and Yu.V.Shmartsev, Consultants Bureau - New York-London, 1971. p.216-223.
11. M. I. Dyakonov, M. E. Levinshtein. Sov. Phys. Semicond., vol. 12, p. 992, (1978).
12. M. I. Dyakonov, M. E. Levinshtein. Sov. Phys. Semicond., vol. 12, p. 426, (1978).
13. M. I. Dyakonov, M. E. Levinshtein. Sov. Phys. Semicond., vol. 14, p. 283, (1980).
14. M.E.Levinshtein, J.W.Palmour, S.L.Rumyantsev, and R. Singh Int. Phys. Conf. Ser. No 155, Chapter 8, Proceedengs of 23rd Intern. Symposium on Compound Semiconductors (ISCS-23), Sept.23-27,1996, St.Petersburg, Russia, pp. 601 - 603.
15. M.E. Levinstein, J.W. Palmour, S.L. Rumyantsev and R. Singh, IEEE Transactions on Electron Devices v. ED-44, No. 7, pp. 1177-1179, (1997).
16. S. N. Vainshtein, Yu. V. Zhilyaev, M. E. Levinshtein, Sov. Phys. Semicond., vol. 21, p. 77, (1987).
17. H. Yamasaki. IEEE Trans. Electron Dev., vol. ED-22, p. 65, (1975).
18. V A. Kuzmin. 1971 *Soverskoe Radio*" Publ Hous., Moscow,
19. N.V. Dyakonova, M.E.Levinshtein, J.W.Palmour, S.L.Rumyantsev, and R.Singh. 4 Intern. Symp. on Semicond. Device Research. (ISDRS-97),Charlottesville, USA, Dec. 10-13, 1997, pp.367-370.
20. N.V. Dyakonova, M.E. Levinshtein, J.W. Palmour, S.L.Rumyantsev, and R. Singh Semicond. Sci. Technol. v.13, no 2, pp. 241-243, (1998).
21. N.V. Dyakonova, M.E. Levinshtein, J.W. Palmour, S.L.Rumyantsev, and R. Singh, MRS Spring Meeting 1998, April 13-17, San Francisco, F5.1, p. 113
22. A.M. Strel'chuk, , Semiconductors, **29**, pp. 614-623, (1995),
23. V.I. Brylevskii,, V.P. Reshetin, and V.B. Shuman, Soviet Phys. Semicond., **11**, pp. 822, (1977).
24. S. N. Vainshtein, Yu.V. Zhilyaev, and M.E. Levinshtein,. Sov. Phys. Techn.Phys., **28**, pp. 788, (1983),]
- 25.. S. N. Vainshtein, I. I. Diakonu, Yu. V. Zhilyaev, M. E. Levinshtein, Sov. Tech. Phys. Lett., vol. **28**, p. 359,(1983.)
26. M.E.Levinshtein, J.W. Palmour, S.L.Rumyantsev, and G.S. Singh, Abstracts of 2nd European Conference on Silicon Carbide and Related Materials. Montpellier, France, Sept. 02-06, 1998, pp. 231-232
27. M.E. Levinshtein, J.W. Palmour, S.L. Rumyantsev, and R. Singh, Semicond. Sci. Technol. v.13, p. 1006, (1998).
28. M.M. Anikin, P.A. Ivanov, A.A. Lebedev, S.N. Pytko, A.M. Strel'chuk, and A.L. Syrkin in "Semiconductor interfaces and microstructures", ed. by Z.C.Feng (World Scientific, Singapore- New Jersey-London, 1992) pp.280-311.
29. M.E. Levinshtein, J. W. Palmour, S. L. Rumyanetsev, and R. Singh., IEEE Trans. on ED v.45, no.1, pp.307-312 (1998)
30. A. Herlet and R. Raithel, Solid State Electronics, v.**11**, p. 717 (1968).
31. R. L. Longini, J. Melngailis. IEEE Trans. Electron Dev., vol. ED-**10**, p. 178, (1963).
32. M.E. Levinshtein, J.W. Palmour, S.L. Rumyantsev and R. Singh, Submitted in: Semicond. Sci. Technol. September 1998.

ANNEX

**Amount of unused funds remaining on the contract at the
end of the period covered by report:**

\$6000